Cell

Single-Molecule mRNA Decay Measurements Reveal Promoter-Regulated mRNA Stability in Yeast

Tatjana Trcek,[1] Daniel R. Larson,[4] Alberto Moldón,[2] Charles C. Query,[2] and Robert H. Singer[1,3,*]
[1]Anatomy and Structural Biology
[2]Cell Biology
[3]Gruss-Lipper Biophotonics Center
Albert Einstein College of Medicine, 1300 Morris Park Avenue, Bronx, NY 10461, USA
[4]National Cancer Institute, National Institutes of Health, 41 Library Drive, Bethesda, MD 20892, USA
*Correspondence: robert.singer@einstein.yu.edu
DOI 10.1016/j.cell.2011.11.051

SUMMARY

Messenger RNA decay measurements are typically performed on a population of cells. However, this approach cannot reveal sufficient complexity to provide information on mechanisms that may regulate mRNA degradation, possibly on short timescales. To address this deficiency, we measured cell cycle-regulated decay in single yeast cells using single-molecule FISH. We found that two genes responsible for mitotic progression, *SWI5* and *CLB2*, exhibit a mitosis-dependent mRNA stability switch. Their transcripts are stable until mitosis, when a precipitous decay eliminates the mRNA complement, preventing carryover into the next cycle. Remarkably, the specificity and timing of decay is entirely regulated by their promoter, independent of specific *cis* mRNA sequences. The mitotic exit network protein Dbf2p binds to *SWI5* and *CLB2* mRNAs cotranscriptionally and regulates their decay. This work reveals the promoter-dependent control of mRNA stability, a regulatory mechanism that could be employed by a variety of mRNAs and organisms.

INTRODUCTION

Precise analysis of decay kinetics is necessary to understand when and how a decay regulator functions, and single-cell, single-molecule techniques could advance our understanding of mRNA turnover. For example, the kinetic behavior of individual RNA polymerase II (RNAPII) transcribing a gene (reviewed in Ardehali and Lis, 2009) provides a precise quantification of the contribution of mRNA synthesis to the cellular pool of transcripts. However, to date, no such approach has been available for measuring mRNA turnover. Traditional techniques have relied on normalization of decay signal and on a large sample of cells, genetically modified or treated with inhibitors, to stop transcription and thus obtain kinetic information of a decaying mRNA species (reviewed in Passos and Parker, 2008). Furthermore, the accuracy of decay measurement varies with the technique used. For example, in budding yeast, half-lives of an individual mRNA species quantified by different approaches may differ by more than 50 percent (Grigull et al., 2004; Holstege et al., 1998; Wang et al., 2002). In turn, the accuracy of the decay curve will influence how precisely it can be modeled. In this work, we use single-molecule counting with fluorescent in situ hybridization (FISH) (Zenklusen et al., 2008) to derive an absolute measure of mRNA synthesis and decay in individual cells. This provided a highly sensitive approach for detecting changes that occur in a fraction of cells and would otherwise have been obscured.

We focused on mRNA turnover because it could regulate gene expression during the cell cycle. For instance, entry into mitosis induces a rapid mRNA decay of the mitotic Clb2p cyclin that, if prevented, can cause failure of cells to finish mitosis (Cai et al., 2002; Gill et al., 2004). Entry into G0 causes stabilization of specific G0 mRNAs (Talarek et al., 2010), whereas the stability of the canonical histone mRNAs increases with the onset of S phase, and exit from S phase induces their rapid decay (Marzluff et al., 2008; Osley, 1991). Thus, together with their cyclical transcription, the destabilization of mRNAs can restrict the activity of periodically expressed genes to a particular cell-cycle phase. This modulation of stability is typically achieved through binding of decay regulators to specific sequences located in the mRNA (reviewed in Guhaniyogi and Brewer, 2001).

We focused on two cell cycle-regulated genes, *SWI5* and *CLB2*, and measured changes in their mRNA turnover during the cell cycle. Swi5p is a transcription regulator of late mitosis genes, and Clb2p is a G2 phase cyclin that drives the progression of cells towards mitosis. They are coregulated through shared promoter elements (Koranda et al., 2000; Spellman et al., 1998; Zhu et al., 2000) and were measured to degrade with 8 min and 4.5 min half-lives, respectively (Wang et al., 2002). We used morphological markers to determine timing of the cell cycle. We counted absolute numbers of cytoplasmic and nascent transcripts (Zenklusen et al., 2008) and analyzed decay rates using a mathematical model without the use of transcriptional inhibitors, genetic mutants, or the need to normalize mRNA signal.

The use of a single-molecule mRNA decay measurement enabled identification of a regulatory pathway of mRNA decay that provides an additional level of cell cycle regulation. We determined that the half-life of *SWI5* and *CLB2* decreases more than 30-fold with the onset of prometaphase/metaphase. Furthermore, regulation of this mRNA decay is coordinated with their transcription and controlled by their promoter sequence, independent of the specific *cis* sequences located in the mRNA. By using morphological markers, we were able to determine that the cell cycle progression and the prometaphase/metaphase stability switch of *SWI5* and *CLB2* were coupled and regulated by the mitotic exit network kinases, Dbf2p and Dbf20p. Both kinases bind to *SWI5* and *CLB2* mRNAs, and Dbf2p is also enriched at their transcription sites. We propose a model whereby Dbf2p is first recruited by the promoter and then cotranscriptionally deposited onto the mRNA. Once in the cytoplasm, the mRNA associates with Dbf20p and then waits for the appropriate cellular cues to initiate the decay process. Thus, for a subset of budding yeast mRNAs, promoter-dependent activity directly influences how and when an mRNA will be degraded in the cytoplasm.

RESULTS

SWI5 and *CLB2* mRNA Exhibit Cell Cycle-Dependent Decay Kinetics

We measured *SWI5* and *CLB2* mRNAs decay rates in exponentially growing cells using the common approaches of qRT-PCR coupled with the transcriptional inhibitor thiolutin. A constitutively expressed *ACT1* was expected to decay independently of the cell-cycle phase with a single decay rate ($t_{1/2}$ of 45 min) (Wang et al., 2002) and was used as a control. Decay curves of *SWI5*, *CLB2*, and *ACT1* (Figures 1A–1C) were fitted to both an exponential decay with a single component (green line) and two components (red line) to identify which kinetic model best described their decay curves. A two-component model detected a decay-resistant *SWI5* mRNA population ($t_{1/2}$ > 90 min) and a rapidly decaying *SWI5* mRNA population ($t_{1/2}$ = 3.0 min), whereas a single component model with a $t_{1/2}$ = 6.9 min showed systematic deviations from the measured data. A two-component model was not able to resolve multiple *CLB2* decay populations and, similarly to *ACT1* mRNA, fitted the decay data as well as a single component model. Here, *CLB2* mRNA decayed with a single $t_{1/2}$ = 3.7 min, whereas *ACT1* mRNA decayed with a single $t_{1/2}$ = 41.3 min, consistent with previously reported values (Wang et al., 2002).

To test whether *SWI5* and *CLB2* mRNAs decayed differently during the cell cycle, we synchronized cells in different cell-cycle phases followed by thiolutin inhibition. In S phase and at G2/M border, *SWI5* and *CLB2* mRNAs were stable, whereas in mitosis, they decayed rapidly with an estimated $t_{1/2}$ of ~3 min (Figures 1D–1G and Figure S1A available online). *ACT1* decayed independently of the cell-cycle phase and, similarly to unsynchronized cells, turned over with a single $t_{1/2}$ of ~30 min.

Kinetics of transcription inhibition by thiolutin was independent of the synchronization protocol (Figure S1B), and thus we could conclude that the stability of *SWI5* and *CLB2* mRNAs, but not of *ACT1* mRNA, changed depending on the cell-cycle phase. Two *CLB2* decay populations, however, could only be detected when physically separated in time by cell culture synchronization. Therefore, normalization of mRNA decay signal, inhibition of transcription, and use of population measurements obscured the behavior occurring in a fraction of cells, thus diminishing the sensitivity of the technique. We employed an approach that was both highly quantitative and minimally invasive to the cell's physiology. We modified a FISH-based method that enabled us to quantify mRNA decay rates in individual, minimally perturbed cells with single mRNA sensitivity without the need for transcription inhibition, cell synchronization, or normalization of mRNA signal.

Measuring mRNA Decay Using Single-Cell, Single-Molecule FISH

We counted single transcripts in the cytoplasm in individual cells using single-cell, single-molecule FISH (Zenklusen et al., 2008). A mix of fluorescently labeled probes hybridizing along an mRNA was used (Figure 2A, red probes, and Table S1), which strongly amplified the signal-to-noise ratio and detection sensitivity. Fluorescent transcripts were detected and counted using the algorithm Localize (Larson et al., 2005; Zenklusen et al., 2008; Figure S2A). Specific fluorescent signal was only detected in the presence of a target mRNA (Figures S2C and S2D). After cell segmentation, we obtained an absolute number of transcripts per cell, which obviated normalization of mRNA signal required for ensemble measurements and thus the uncertainty associated with them.

FISH probes also annealed to the nascent chains whenever a cell actively transcribed a gene. We used a single probe targeted to the 5′-most end of the transcript labeled with a spectrally distinct fluorophore (Figures 2A, green probe, and S2B) and quantified the number of these probes annealed at the site of transcription (Femino et al., 1998; Zenklusen et al., 2008). This approach constitutes a direct measure of transcriptional activity in the cell, and the number of nascent chains reflects both the transcript initiation rate and the dwell time of a transcript as determined by all postinitiation processes, including elongation and termination (see below). By directly measuring this transcriptional output, transcription inhibition was no longer needed, which enabled us to measure kinetics of mRNA decay in chemically unperturbed cells.

To quantify changes in mRNA stability through mitotic division, we binned cells into cell-cycle phases using morphological markers as indicators of cell-cycle time (Brewer et al., 1984; Hartwell, 1974; Lord and Wheals, 1980; Figure 2B). This approach provided temporal resolution without the need for cell synchronization. Four morphological markers were used: bud size (DIC), movement of the nucleus detected by DAPI, positioning of the spindle pole body indicated by CFP-tagged Spc42p, and localization of a GFP-tagged Whi5p. Whi5p is nuclear during telophase, cytokinesis, and G1 phase of the cell cycle and is cytoplasmic in all others (Bean et al., 2006), allowing differentiation between G1 phase and early S phase cells that have not yet formed a bud. Duplication time of the yeast culture was 90 ± 8.5 minutes, and the percent of cells in each phase was directly proportional to its length in minutes. For example, 18.3% of cells were identified as late S phase cells, which

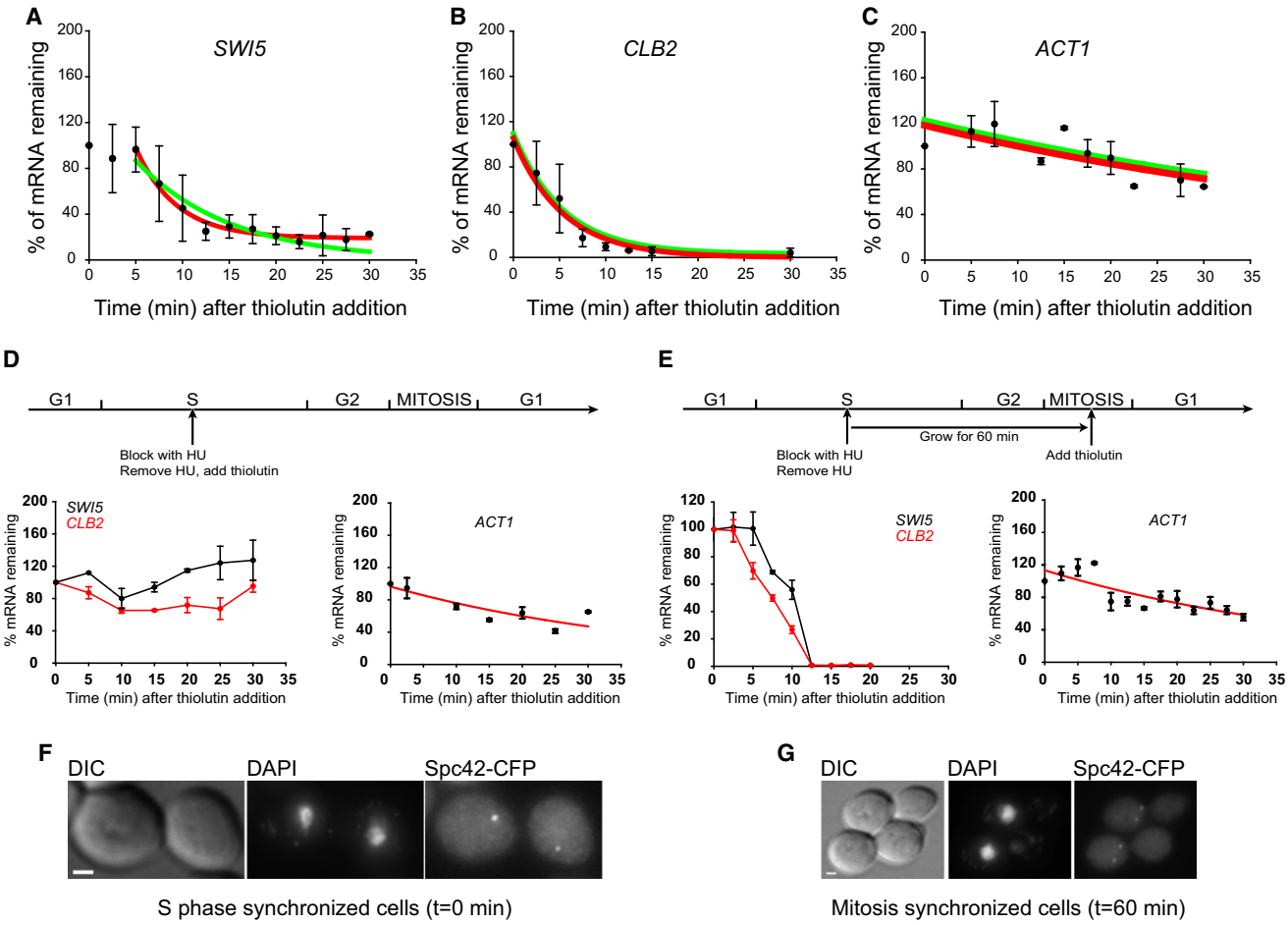

Figure 1. Stability of *SWI5* and *CLB2* Changes with the Cell-Cycle Phase

(A–C) Thiolutin was added to exponentially growing cells, and relative mRNA levels were measured using qRT-PCR. (Green line) Decay curves fitted to an exponential decay with a single component; *SWI5* $t_{1/2}$: 6.9 ± 1.0 min (R^2 = 0.87); *CLB2* $t_{1/2}$: 3.7 ± 0.5 min (R^2 = 0.96); *ACT1* $t_{1/2}$: 41.3 ± 14.5 min (R^2 = 0.57). (Red line) Decay curves fitted to an exponential decay with two components; *SWI5* $t_{1/2}{}^1$: 3.0 ± 0.9 min and $t_{1/2}{}^2$ > 90 min (R^2 = 0.98); *CLB2* $t_{1/2}{}^1 = t_{1/2}{}^2$: 3.7 min ($R^2$ = 0.96); *ACT1* $t_{1/2}{}^1 = t_{1/2}{}^2$: 41.0 min ($R^2$ = 0.57).

(D and E) Cells were synchronized in S phase with hydroxyurea (HU) and mRNA decay measured after thiolutin was added. For measurements in mitosis, cells were removed from the cell-cycle block and grown for 1 hr, and then thiolutin was added and mRNA decay measured (Gill et al., 2004). In S phase, *SWI5* and *CLB2* were decay resistant. *ACT1* $t_{1/2}$: 29.0 ± 8.2 min (R^2 = 0.74), and in M phase, *SWI5* and *CLB2* decayed with $t_{1/2} \sim 3$ min. *ACT1* $t_{1/2}$: 31.5 ± 8.3 min (R^2 = 0.67). In all panels, an average of two experiments with SD is shown.

(F and G) Cells synchronized with HU in S phase (t = 0 min) and mitosis (t = 60 min). Images of DIC, nucleus (DAPI), and a spindle pole body marker (Spc42-CFP) are shown.

Scale bars, 1 μm. See also Figure S1.

converted to 16.5 min (Figure 2B). Cell binning was highly reproducible among experiments using the same strain, with a variability ≤10%. Thus, one can determine the relative time of progression through the cell cycle, allowing one to obtain dynamics of cell-cycle gene expression from a population of fixed cells.

SWI5 and *CLB2* mRNA Stability Are Coordinated with Transcription

As anticipated for coregulated genes, expression of *SWI5* and *CLB2* was similar and followed four discernable stages (Figures 3A–3D). The first spanned the entire S phase, when transcription was infrequent and mRNA accumulation modest. The second stage spanned G2 phase and prometaphase/metaphase, when transcription increased sharply and the bulk of mRNA synthesis occurred within 6.7 minutes. The onset of the third phase coincided with the onset of anaphase. Transcription of both genes ceased, and transcripts were degrading rapidly. In the last stage during G1 phase, the probability of expression of either of the genes fell below 5%.

Because transcription became inactive during mitosis, mRNA decay rates could be determined directly from their cytoplasmic mRNA profiles (Figures 3C and 3D, blue line). During mitosis, *SWI5* and *CLB2* mRNAs decayed with a $t_{1/2}$ of 2.1 ± 0.8 min and a $t_{1/2}$ of 1.8 ± 0.5 min, respectively, based on the fit to the cellular RNA profiles. This rapid decay prevented carryover of mRNAs into the new cell cycle (demarcated with gray boxes).

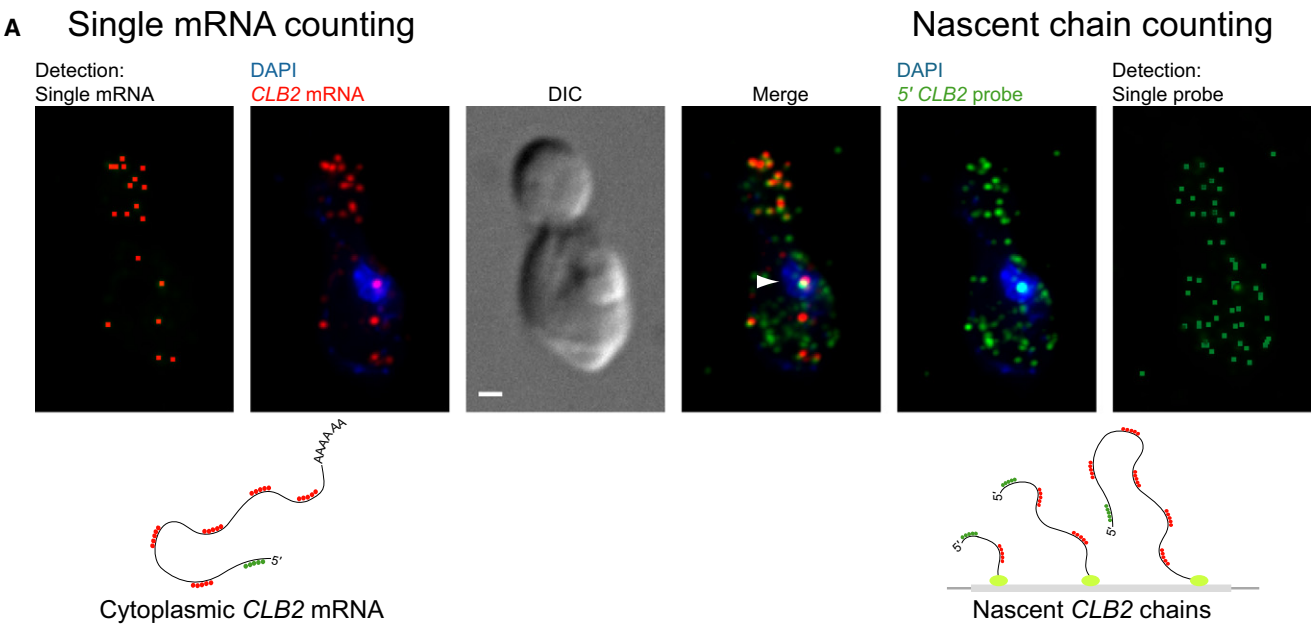

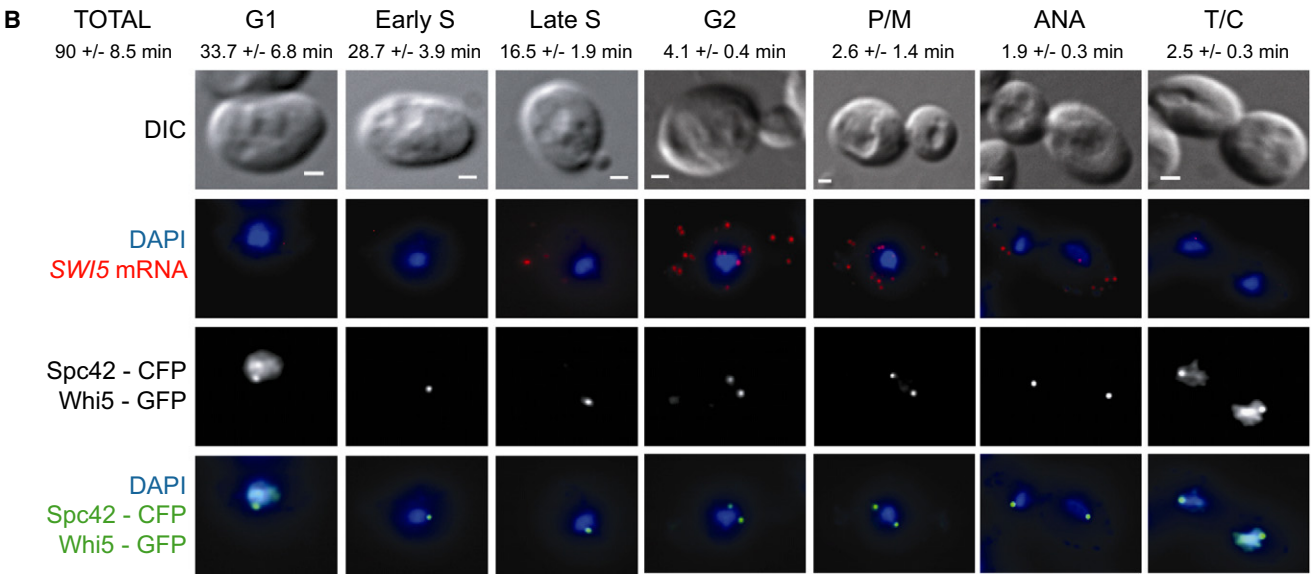

Figure 2. Measuring mRNA Decay Rates Using Single-Cell, Single-Molecule FISH

(A) (Red) A mix of cy3.5-labeled probes was used to count single cytoplasmic transcripts. (Green) A 5′-most cy3-labeled probe was used to count the number of nascent chains at the transcription site (arrowhead).

(B) Morphological markers used to bin cells into cell cycle phases: G1, early S, late S, G2, prometaphase/metaphase (P/M), anaphase (ANA), and telophase/cytokinesis (T/C). An average cell-cycle phase length between two experiments ± SD is shown. Minimally, 600 cells per experiment were counted, and the length of each phase in minutes was calculated.

Scale bars, 1 μm. See also Figure S2.

Decay rates previously observed for *SWI5* and *CLB2* (Wang et al., 2002) were inconsistent with the data obtained by FISH; the slower decay rate would have contaminated the next cycle (Figures 3C and 3D, green line).

To quantify *CLB2* and *SWI5* decay rates in the context of changing transcriptional activity during the cell cycle, we used mathematical modeling. The number of cytoplasmic mRNAs at any point of the cell cycle depends on the rates of their synthesis and decay. By measuring the total transcript level and the synthesis rate, we can determine the decay rate constant according to the differential equation:

$$\frac{dN}{dt} = \frac{m}{T} - kN \qquad (1)$$

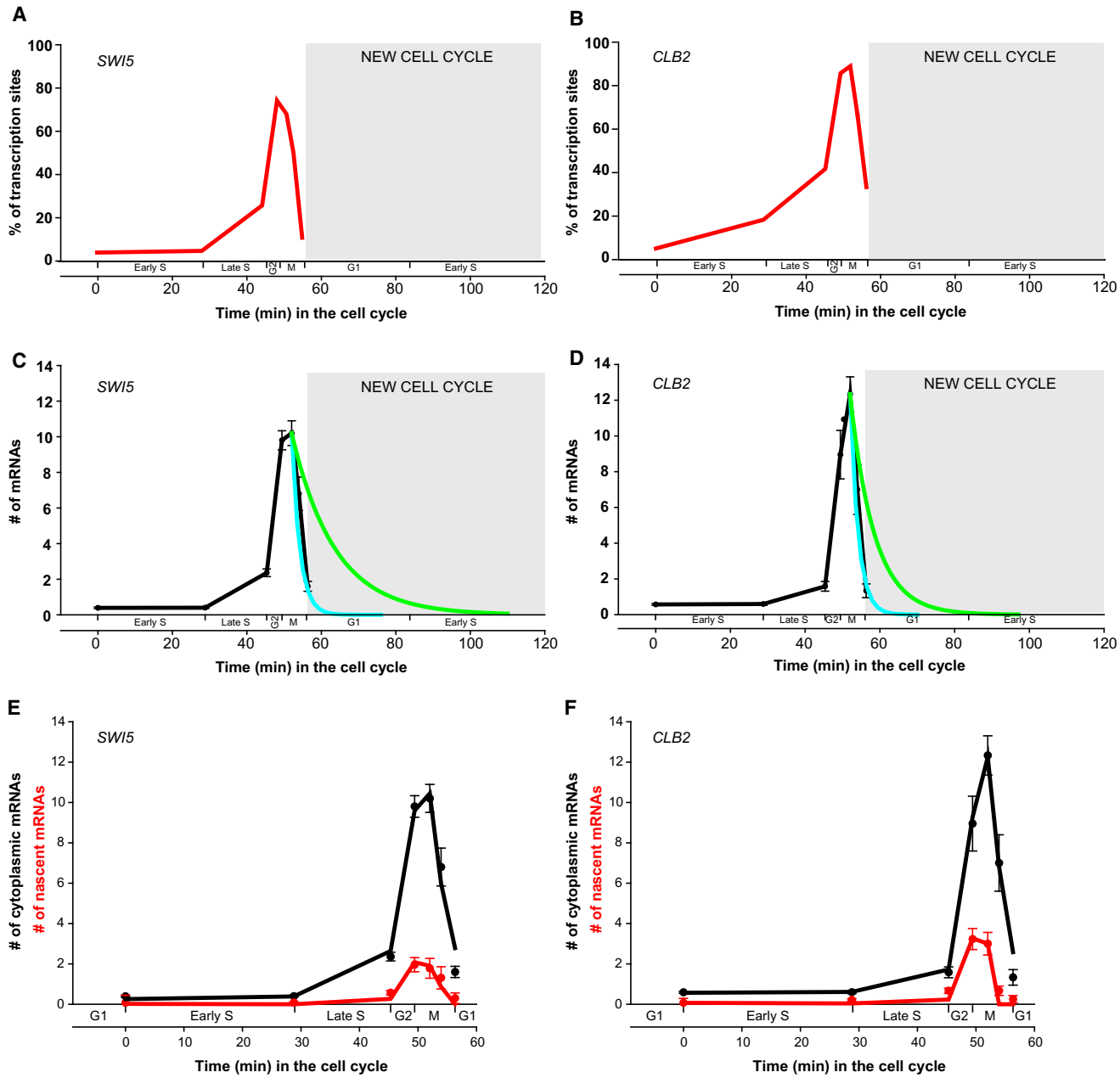

Figure 3. Decay of *SWI5* and *CLB2* mRNAs Is Coordinated with Transcription

(A and B) Percentage of cells with a *SWI5* or *CLB2* transcription site per cell-cycle phase.

(C and D) Determining the mitotic decay constant. (Black lines and circles) Number of cytoplasmic *SWI5* and *CLB2* mRNAs/cell (*N*) ± SEM determined by FISH. (Blue curve) Cytoplasmic *SWI5* and *CLB2* mRNA profiles fitted to a single exponential decay model whereby, during mitosis, *SWI5* and *CLB2* decayed with a $t_{1/2}$ of 2.1 ± 0.8 min ($R^2 = 0.94$) and $t_{1/2}$ of 1.8 ± 0.5 min ($R^2 = 0.97$), respectively. (Green line) *SWI5* and *CLB2* decay curve from published literature with $t_{1/2} = 8$ min and $t_{1/2} = 4.5$ min, respectively (Wang et al., 2002). Gray boxes demarcate a new cell cycle.

(E and F) Quantifying the premitotic decay constant using the mathematical model. (Black circles) As in A and B. (Red circles) Number of *SWI5* and *CLB2* nascent mRNAs/cell (*m*) ± SEM determined by FISH. (Black line) Mathematical fit to *N*. (Red line) Mathematical fit to *m*. For *SWI5* $T = 66 \pm 7.0$ s, a premitotic $t_{1/2} > 90$ min and a mitotic $t_{1/2} = 2.1$ min ($\chi^2 = 31.5$). For *CLB2* $T = 63 \pm 5.5$ s, a premitotic phase $t_{1/2} = 66$ min, and a mitotic $t_{1/2} = 1.8$ min ($\chi^2 = 50.0$).

In all graphs, x axis delineates duration of each cell-cycle phase (min). M includes P/M, ANA, and T/C. See also Figure S3.

where *N* is the number of transcripts in the cytoplasm (Figure 2A); *t* is time; *m* is the transcriptional activity of a gene measured by the number of nascent transcripts at a transcription site (Figure 2A); *T* is the dwell time of a nascent transcript (s); and *k* is the degradation rate constant (s^{-1}) (see Experimental Procedures). The solution to this differential equation is:

$$N(t) = \frac{m}{kT}\left(1 - e^{-kt}\right) + N_0 e^{-kt} \quad (2)$$

where N_0 is the initial number of transcripts. The time t is determined from cell-cycle markers as described above (Figure 2B). The measured values are m and N determined as a function of t, and the fit parameters are k and T. For each gene, a global nonlinear least-square fit to the expression profile was determined.

This model describes RNA levels as a balance of zero-order RNA synthesis and first-order decay. We assume first-order mRNA decay because it is the simplest model that describes our data and allows us to compare to bulk biochemical measurements of mRNA stability. In the simplest form, with a dwell time and an mRNA half-life that are invariant over the cell cycle, both fit values are < 35 s, resulting in RNA polymerase velocities and RNA lifetimes that are unphysical (Figures S3A–S3G). However, if we include the possibility of bimodal decay, as experimentally observed in Figure 1, the model captures the essential features of *SWI5* and *CLB2* regulation over the cell cycle. We kept the mitotic $t_{1/2}$ fixed at 2.1 min for *SWI5* and $t_{1/2}$ at 1.8 min for *CLB2,* as determined by the FISH measurements (Figures 3C and 3D and S3C–S3G), and allowed the nascent transcript dwell time and the premitotic decay to float. This fitting regime reached a global minimum with the following parameter values: for *SWI5* mRNA, a dwell time of 66 ± 7.0 s and a premitotic $t_{1/2} > 90$ min (Figure 3E, solid lines) and for *CLB2* mRNA a dwell time of 63 ± 5.5 s and a premitotic $t_{1/2}$ of 66 min (Figure 3F, solid lines). The dwell times consist of elongation and postelongation processes, and if the termination time is estimated as 30 s (Zenklusen et al., 2008), the resulting polymerase velocity is ~50 bp/s, consistent with the polymerase velocity of 46 ± 6.2 bp/s during S/G2/M (Larson et al., 2011). Additionally, the bimodal decay kinetics is invariant of nascent chain dwell times as long as these remain within the physiological boundaries of $T > 18$ seconds (Figures S3C–S3G). Lastly, based on the best fit of our model, we determined that the switch in mRNA stability occurred during prometaphase/metaphase, when transcription for both genes was at its peak, even though the rapid decay became apparent only with the onset of anaphase, when transcription was shutting down (Figures 3A–3F).

To further address the timing of destabilization, we modeled the data assuming that the switch in mRNA stability occurred with the onset of anaphase. This fitting regime also resulted in bimodal decay kinetics similar to the one described above but with the higher divergence of the mathematical fit from the FISH data (data not shown). Based on the best fit criterion, this anaphase-specific model was thus not considered in the analysis of *SWI5* and *CLB2* decay kinetics.

Several important conclusions are evident: (1) prior to mitosis, *SWI5* and *CLB2* transcripts were stable, allowing the cell to increase mRNA levels during active transcription; (2) during mitosis, when *SWI5* and *CLB2* transcription were shutting down, their transcripts decayed rapidly, preventing carryover into the next cell cycle; (3) the switch from one state to the other occurred during prometaphase/metaphase (P/M), when *SWI5* and *CLB2* transcription reached its peak. These data suggest, therefore, that mRNA synthesis and decay were temporally coordinated for *SWI5* and *CLB2*.

The Promoter Regulates *SWI5* mRNA Stability

We sought to characterize the mechanisms that control the cell cycle-dependent decay. Several regulatory elements could control degradation of an mRNA: its 5′ and 3′UTRs, its ORF, or its promoter. We thus replaced the *SWI5* 5′ and 3′UTRs and the promoter sequence with the corresponding regions of constitutively expressed *ACT1* and *DOA1* genes. We constructed cloning cassettes that allowed the integration of the constructs into the native *SWI5* locus with a concurrent deletion of WT *SWI5* copy (Figure 4A and Table S3). In wild-type cells, *ACT1* mRNA demonstrated a single decay rate of 41.5 min (Figures 1C–1E) and accumulated transcripts throughout mitosis, unlike *SWI5* (Figure 4B). WT *DOA1* mRNA decayed with a $t_{1/2}$ of 11.0 min and, similarly to *ACT1*, accumulated transcripts throughout mitosis (Figures 4C, S3G, and S4A).

We tested the influence of *SWI5* 5′ and 3′UTRs on the stability of *SWI5* mRNA by replacing them with the 5′ and 3′UTRs of the *ACT1* gene (Figures 4D and S4B). If binding of decay regulators to sequences in 5′ or 3′UTR alone regulated *SWI5* mRNA turnover, then this replacement should abolish cell cycle-dependent mRNA decay and cause continuous accumulation of transcripts similar to WT *ACT1* mRNA. However, this replacement had no effect on either the stability of the chimeric *SWI5* mRNA or the prometaphase/metaphase-specific switch in mRNA stability. As in WT cells, chimeric *SWI5* mRNAs were decay resistant prior to mitosis ($t_{1/2} > 90$ min) and decay sensitive during mitosis ($t_{1/2}$ =2.4 ± 1.3 min).

We then replaced only the *SWI5* promoter with that of *ACT1* while keeping the rest of the *SWI5* mRNA intact (Figures 4E and S4C). In this strain, *SWI5* transcripts showed expression profiles similar to *ACT1*, with a single half-life of 19.7 min and continuous accumulation of transcripts throughout mitosis. Furthermore, when in addition to the *SWI5* promoter we also changed its 5′ and 3′UTR for that of *ACT1* gene (Figure S4D), *SWI5* transcripts decayed with a single decay rate of 18.7 min throughout the cell cycle.

In the reciprocal experiment, rapid decay during mitosis would bring *ACT1* mRNA below the critical amount needed for the cell to survive. Therefore, we used the nonessential *DOA1* gene, which decays similarly to *ACT1* (Figures 4C and S4A) and expressed it using a *SWI5* promoter (Figures 4F and S4E). Under *SWI5* promoter control, cell cycle-dependent transcription and decay of *SWI5* mRNA were recapitulated on *DOA1* mRNA. *DOA1* mRNAs were stable prior to mitosis, with a $t_{1/2} > 90$ min, and decayed rapidly, with a $t_{1/2}$ of 4.9 ± 0.7 min during mitosis. Therefore, changes in the mRNA stability through the cell cycle were regulated entirely by *SWI5* promoter and were independent of the specific *cis* mRNA sequences.

The Promoter Also Regulates *CLB2* mRNA Stability

The same transcription factors that regulate *SWI5* expression also regulate *CLB2* expression (Darieva et al., 2006; Koranda et al., 2000; Spellman et al., 1998; Zhu et al., 2000), and thus it was likely that, as with *SWI5*, the cell cycle-dependent decay of *CLB2* was also controlled by its promoter. We thus replaced the promoter of *CLB2* for that of *ACT1* while keeping the rest of the *CLB2* mRNA intact. When expressed from the *ACT1* promoter, *CLB2* transcripts turned over with a single mRNA

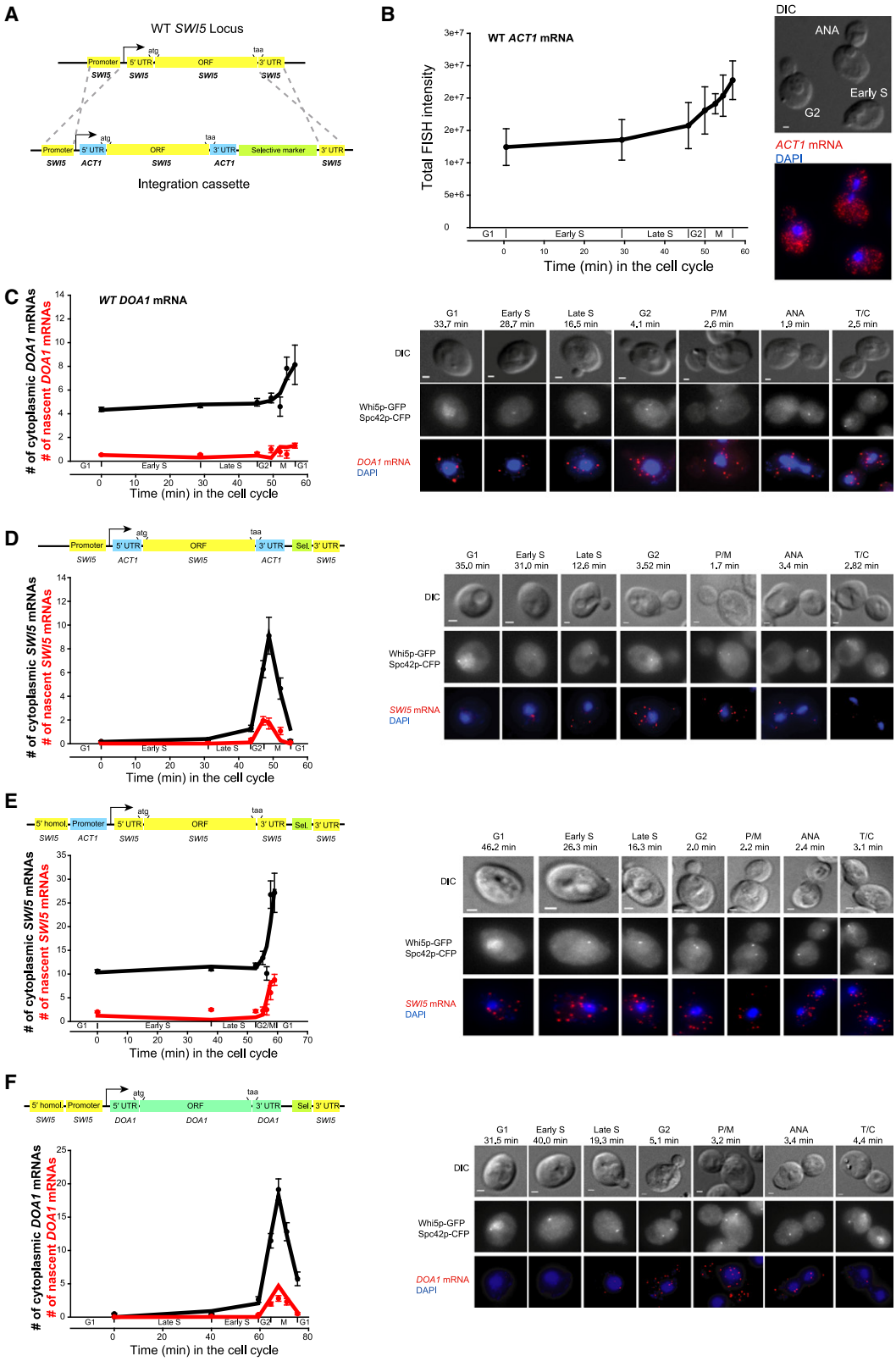

Figure 4. *SWI5* mRNA Decay Is Determined by Its Promoter

(A) Design of an integration cassette. Colors denote gene origins: *SWI5*, yellow; *ACT1*, blue; *DOA1*, pale blue; selection marker, green.

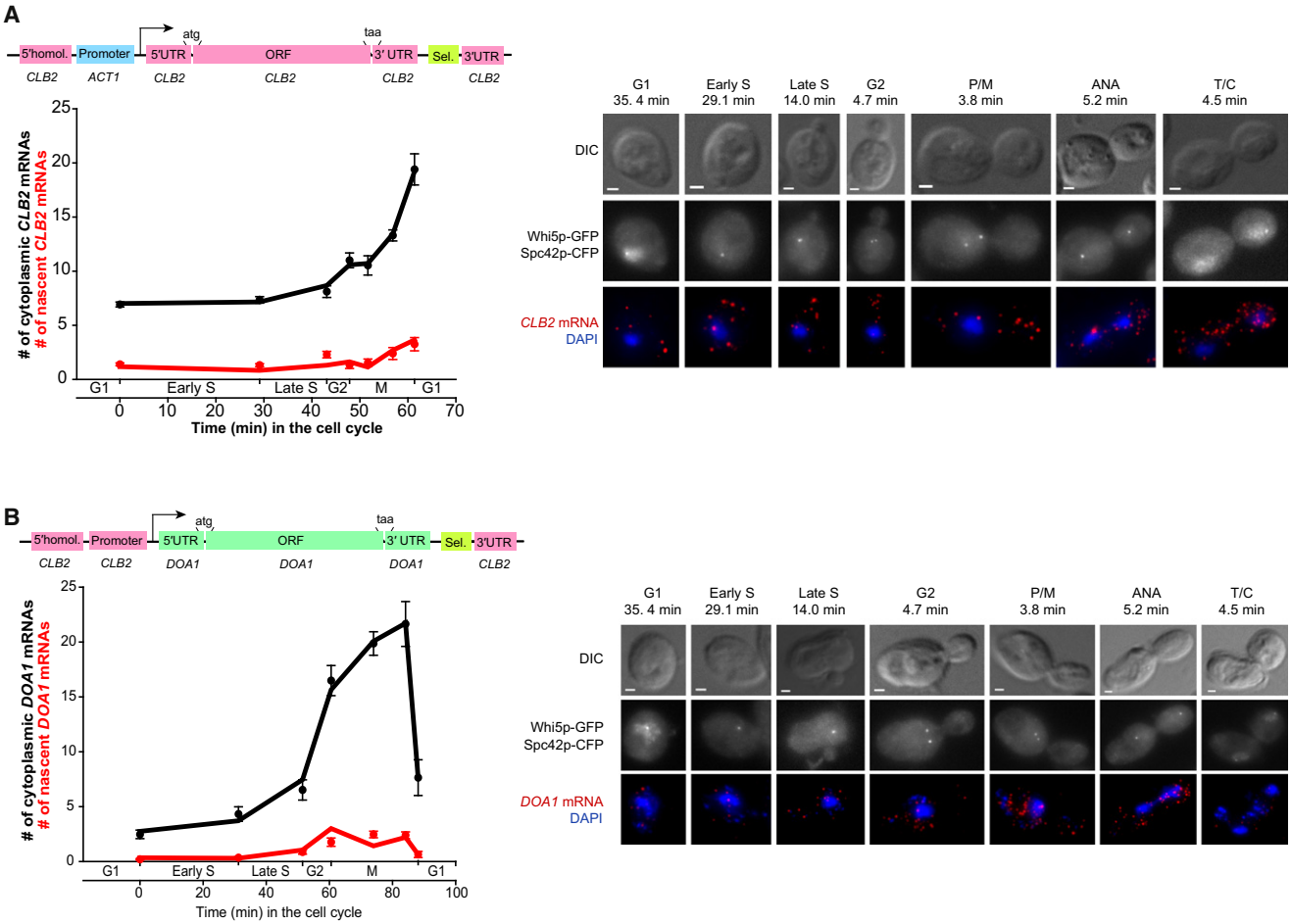

Figure 5. *CLB2* mRNA Decay Is Determined by Its Promoter

(A and B) An integration cassette used to create the strain is shown. Colors denote gene origins: *ACT1*, blue; *DOA1*, pale blue; *CLB2*, violet; selection marker, green. (Black circles) Number of cytoplasmic *CLB2* or *DOA1* mRNAs/cell (*N*) ± SEM determined by FISH; (red circles) Number of *CLB2* or *DOA1* nascent mRNAs/cell (*m*) ± SEM determined by FISH; (black line) mathematical fit to *N*; (red line) mathematical fit to *m*.

(A) *CLB2* mRNA expressed from the *ACT1* promoter: $T = 66$ s and a $t_{1/2}$ of 4.9 min ($\chi^2 = 32.4$).

(B) *DOA1* mRNA expressed from the *CLB2* promoter: $T = 77$ s, a pretelophase/cytokinesis $t_{1/2}$ of 14.7 min, and a telophase/cytokinesis $t_{1/2}$ of 0.9 min ($\chi^2 = 32.5$). In all graphs, the x axis delineates duration of each cell-cycle phase (min). M includes three cell-cycle phases: P/M, ANA, and T/C. Images of cells through the cell cycle are shown. Scale bars, 1 μm.

half-life of 4.9 min and, unlike WT *CLB2* mRNAs, accumulated continuously throughout mitosis (Figure 5A).

In the reciprocal experiment, a constitutively transcribed *DOA1* was expressed from the *CLB2* promoter and its mRNA stability measured. In this strain, the gene expression features of *CLB2* were recapitulated on *DOA1*, with a slow mRNA turnover prior to mitosis ($t_{1/2}$ of 14.7 min) and a rapid turnover during mitosis ($t_{1/2}$ of 0.9 min) (Figure 5B). Unlike WT *CLB2*, however, the switch in the *DOA1* mRNA stability occurred during telophase/cytokinesis. Due to the integration of cloning cassette

(B) WT *ACT1* expression over the cell cycle. Note the increase in transcription and transcripts after gene duplication. Summed fluorescence intensity ± SD is shown with images of *ACT1*-expressing cells (see Experimental Procedures).

(C) WT *DOA1*. (Black circles) *N* ± SEM; (red circles) *m* ± SEM quantified by FISH; (black line) mathematical fit to *N*; (red line) mathematical fit to *m*. *T* of 68 s, $t_{1/2} = 11.0$ min ($\chi^2 = 46.7$).

(D–F) Swapping of *SWI5* regulatory sequence elements with *ACT1* and *DOA1* shows that the promoter is the determinant of decay. (Black circles) *N* ± SEM; (red circles) *m* ± SEM quantified by FISH; (black line) mathematical fit to *N*; (red line) mathematical fit to *m*.

(D) Chimeric *SWI5* with *ACT1* 5′ and 3′UTR. *T* of 64 s, a premitotic $t_{1/2} > 90$ min ($\chi^2 = 25.7$), and a mitotic $t_{1/2} = 2.4 \pm 1.3$ min ($R^2 = 0.92$).

(E) *SWI5* with *ACT1* promoter: *T* of 72 s and a $t_{1/2} = 19.7$ min ($\chi^2 = 162.1$).

(F) *DOA1* with *DOA1* 5′ and 3′UTRs expressed from a *SWI5* promoter. *T* of 68 s, a premitotic $t_{1/2} > 90$ min ($\chi^2 = 109.9$), and a mitotic $t_{1/2} = 4.9 \pm 0.7$ min ($R^2 = 0.99$). For (B)–(F), see Experimental Procedures and Table S3. In all graphs, the x axis delineates duration of each cell-cycle phase (min). M includes P/M, ANA, and T/C. Images of cells through the cell cycle for each strain are shown. Scale bars, 1 μm. See also Figure S4.

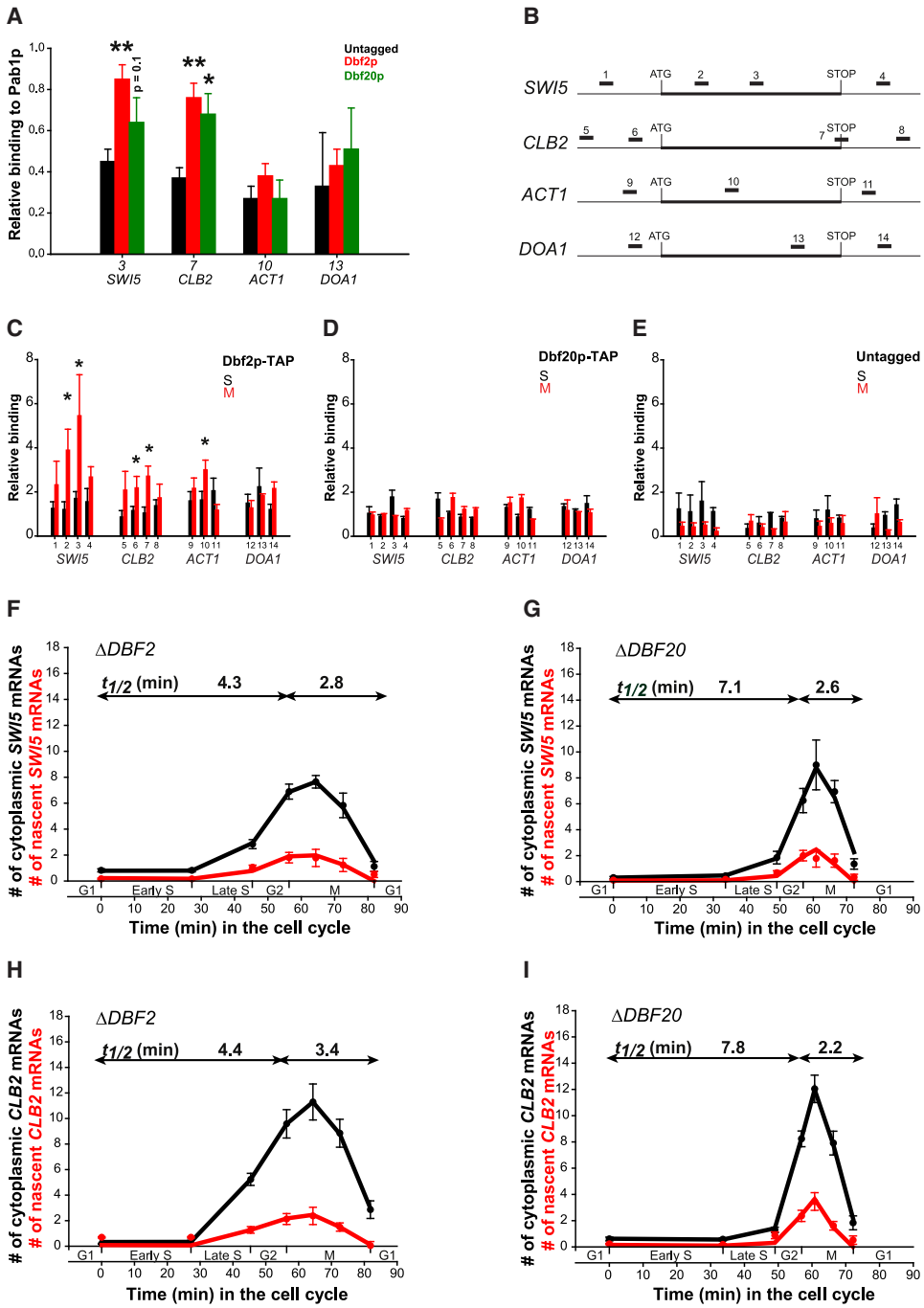

Figure 6. Dbf2p, but Not Dbf20p, Associates with *SWI5* and *CLB2* mRNA during Transcription and Regulates Their mRNA Stability

(A) RNA immunoprecipitation of *SWI5* and *CLB2* mRNAs with Dbf2p-TAP and Dbf20p-TAP from mitotic cells. Binding relative to Pab1p-TAP is shown. Significant enrichment relative to untagged cells is indicated (t test; *p<0.05 and **p<0.01).

(B) The positions of PCR amplicons used in (A)–(E) for each gene are depicted (Table S5).

(C–E) Dbf2p-TAP, Dbf20p-TAP, and an untagged control were immunopurified from S phase (S, black bars) or mitotic cells (M, red bars). Association of these proteins to various regions of *SWI5*, *CLB2*, *ACT1*, and *DOA1* genes was analyzed by qPCR. Data are represented as relative to binding to *TEL V*, a telomeric region in chromosome V. In each panel, an average of three experiments with the SEM is shown. Significant enrichment relative to the S phase cells is indicated (t test; * p<0.05).

(F–I) Dbf2p and Dbf20p deletions affect *SWI5* and *CLB2* mRNA stability. (Black circles) *N* ± SEM; (red circles) m ± SEM; (black line) mathematical fit to *N*; (red line) mathematical fit to *m*.

(F) *SWI5* in Δ*DBF2*: *T* of 66 s, premitotic $t_{1/2}$ = 4.3 min, and a mitotic $t_{1/2}$ = 2.8 min (χ^2 = 6.3).

into the *CLB2* locus, this strain did not express the Clb2 cyclin. Consistent with the literature, this deletion resulted in an abnormal cell cycle and a delayed progression through mitosis (Figure 5B; Fitch et al., 1992), which could have adverse effects on the decay process and the timing of the *DOA1* mRNA stability switch.

These results demonstrate that the promoter sequence regulates the cell cycle-dependent mRNA turnover of both the *SWI5* and *CLB2*, independent of their *cis* mRNA sequences. mRNA stabilities measured for *SWI5* and *CLB2* when driven from the *ACT1* promoter thus represent their ''innate'' abilities to resist decay. For *SWI5* and *CLB2*, therefore, transcription and mRNA decay are codependent processes in which the regulation of the first influences the outcome of the latter.

mRNA Stability of *SWI5* and *CLB2* Is Regulated by Dbf2p and Dbf20p

A bona fide regulator of *SWI5* and *CLB2* decay requires interaction with their transcription factors, the mRNA decay regulators, and the cell-cycle machinery to ensure coordination among the three. In the search of this *trans*-acting factor, we made use of the *Saccharomyces* genome database. Because the regulation of *SWI5* and *CLB2* decay is promoter dependent, we asked whether any of their transcription factors physically interacted with a protein that, in turn, interacted with the mRNA decay regulators and the cell-cycle regulators to provide coupling among the three processes (see Experimental Procedures). Dbf2p, a mitotic exit network (MEN) kinase, was the only protein that satisfied this criterion. It interacts with Cdc5p (Visintin and Amon, 2001), a *SWI5* and *CLB2* transcription factor and itself a MEN regulator (Darieva et al., 2006); it is a part of a larger CCR4-NOT complex (Liu et al., 1997), a major deadenylase of cytoplasmic mRNAs in yeast (Tucker et al., 2001); and Dbf2p is mitotically active to ensure telophase to G1 phase transition (Toyn and Johnston, 1994). Similarly, Dbf20p performs several Dbf2p functions and is synthetically lethal with Dbf2p (Toyn et al., 1991), so we assayed its role in regulation of *SWI5* and *CLB2* mRNA decay as well.

By using an RNA immunoprecipitation assay and mitosis-synchronized cells to enrich for the *SWI5* and *CLB2* expression, we detected specific and significant binding of TAP-tagged Dbf2p to *SWI5* and *CLB2* mRNAs at levels similar to Pab1p-TAP, but not to *ACT1* and *DOA1* mRNAs (Figures 6A and 6B). Significant Dbf20p-TAP binding was detected only with *CLB2* mRNA. Furthermore, by using chromatin immunoprecipitation (ChIP), we detected significant enrichment of Dbf2p-TAP at *SWI5* and *CLB2* transcriptional units, which was also RNA dependent (Figures 6B, 6C, 6E, and S5A). Dbf2p-TAP binding was only detected in cells enriched in mitosis (red bars) and not in S phase (black bars). This result was anticipated because, in S phase, transcription of *SWI5* and *CLB2* was infrequent (Figures 3E and 3F, red line), and thus the ChIP enrichment was not expected. Accordingly, the RNAPII ChIP in S phase cells was only marginally higher relative to background, particularly for *SWI5* (Figure S5B). Cotranscriptional binding of Dbf20p-TAP to *SWI5* and *CLB2* mRNAs could not be detected (Figures 6B, 6D, and 6E), indicating that Dbf20p interacts with *CLB2* after transcription is completed, possibly in the cytoplasm.

Finally, we measured *SWI5* and *CLB2* mRNA stabilities in the absence of Dbf2p and Dbf20p. Protein levels of either kinases do not fluctuate through the cell cycle (data not shown) (Visintin and Amon, 2001), and hence we speculated that Dbf2p or Dbf20p could regulate either stable or unstable *SWI5* and *CLB2* mRNAs. Deletion of either of the kinases had no effect on the stability of *ACT1* mRNA (Figures S5C and S5D) but greatly affected the stability of *SWI5* and *CLB2* mRNAs, particularly prior to mitosis (Figures 6F–6I). Moreover, the regulation of mRNA stability by Dbf2p was independent of its kinase activity (Figures S5E and S5F). The mRNA half-lives determined for these two mRNAs using thiolutin and qRT-PCR were kinetically inconsistent with the FISH measurements (Figures S5G–S5L). These discrepancies are likely to have occurred due to toxic effects that thiolutin exerts on the physiology of a cell and on the mRNA turnover (Jimenez et al., 1973; Pelechano and Pérez-Ortín, 2008), thus artificially prolonging their mRNA stabilities.

Additionally, both deletions prolonged the G2 to T/C length of the cell cycle relative to the WT by 2- to 4-fold (Figures S6A–S6D), consistent with the literature (Liu et al., 1997). Thus, cells spent a longer time expressing *SWI5* and *CLB2* with transcriptional amplitudes similar to the WT cells but without excessive accumulation of transcripts (red circles in Figures 6F–6I, 3E, and 3F). The measured reduced stabilities of *SWI5* and *CLB2* in *ΔDBF2* and *ΔDBF20* could not have been an artificial consequence of the redistribution of the transcripts over a longer cell cycle because the model accounted for the ongoing transcription. Thus, due to decreased stability of *SWI5* and *CLB2*, cells were estimated to synthesize up to three times more mRNAs to reach the WT levels (Figures S6E–S6H).

These results imply that Dbf2p is recruited to *SWI5* and *CLB2* promoters and loaded onto *SWI5* and *CLB2* nascent chains cotranscriptionally. Dbf2p is then exported with the mRNAs into the cytoplasm, where along with Dbf20p, it regulates the timing of *SWI5* and *CLB2* decay (Figure 7). Dbf2p and Dbf20p thus coordinate between *SWI5* and *CLB2* transcription and mRNA decay and communicate the cell-cycle cues onto the decay machinery to initiate the decay process.

DISCUSSION

Single-Cell, Single-Molecule mRNA Decay Measurements

In this work, we developed a single-cell, single-molecule approach that enabled us to characterize the kinetics of mRNA decay with a high temporal resolution. This approach uncovered a unique promoter-dependent regulatory mechanism of mRNA decay that could be employed by a variety of cell cycle-regulated

(G) *SWI5* in Δ*DBF20*: *T* of 66 s, premitotic $t_{1/2}$ = 7.1 min, and a mitotic $t_{1/2}$ = 2.6 min (χ^2 = 18.9).
(H) *CLB2* in Δ*DBF2*: *T* of 63 s, premitotic $t_{1/2}$ = 4.4 min, and mitotic $t_{1/2}$ = 3.4 min (χ^2 = 115.7).
(I) *CLB2* in Δ*DBF20*: *T* of 63 s, premitotic $t_{1/2}$ =7.8 min, and a mitotic $t_{1/2}$ = 2.2 min (χ^2 = 40.3).
In all graphs, the x axis delineates duration of each cell-cycle phase (min). M includes P/M, ANA, and T/C. See also Figures S5and S6 .

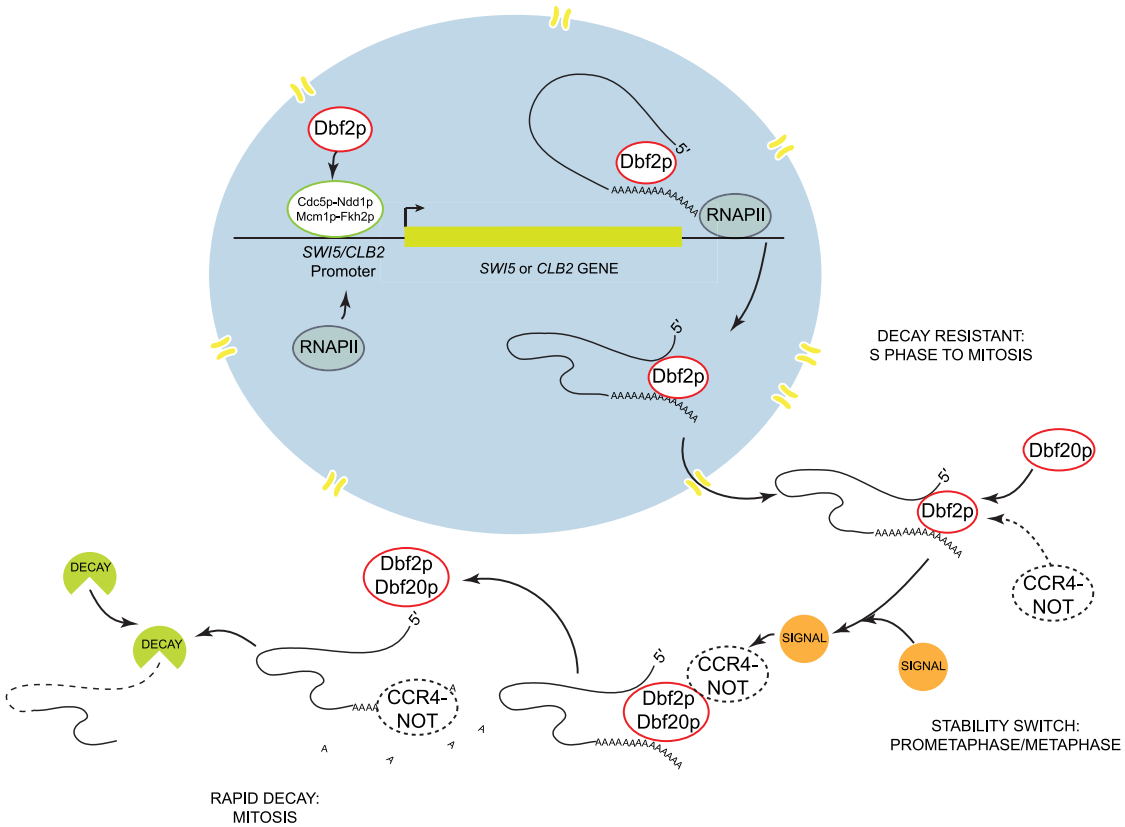

Figure 7. Model Proposing the Life Path of *SWI5* and *CLB2* mRNAs

Dbf2p is recruited to the *SWI5* and *CLB2* promoters and is cotranscriptionally deposited onto *SWI5* and *CLB2* mRNAs. Once exported into the cytoplasm, *SWI5* and *CLB2* mRNA stability is additionally maintained by Dbf20p. During mitosis, Dbf2p is dephosphorylated (Toyn and Johnston, 1994), which could be a cell-cycle progression signal to initiate decay possibly through regulation of the CCR4-NOT complex and deadenylation of the transcripts.

genes. We further identified two regulators of mRNA decay, Dbf2p and Dbf20p, each with distinct functions in regulating *SWI5* and *CLB2* stability. A particular advantage of our approach was that, unlike traditional techniques used to quantify mRNA turnover, we were able to measure transcription and decay concurrently. This enabled us to determine that *SWI5* and *CLB2* transcription and decay were temporally coordinated through the cell cycle. Furthermore, deletion of Dbf2p and Dbf20p resulted in destabilization of *SWI5* and *CLB2* mRNAs and also reduced the efficiency of coordination between transcription and decay. Thus, cells spent a longer time transcribing *SWI5* and *CLB2* without excessive accumulation of mRNAs. To compensate for the increased decay, cells were estimated to synthesize up to three times more mRNAs to reach the WT levels. Our measurements reveal, therefore, that balancing infrequent transcription with mRNA stability is necessary for effective transcript build-up, and transcription shutdown during mitosis and rapid decay prevent carryover of mRNAs into the next cell cycle.

Promoter Regulation of mRNA Decay and Mitotic Division

Achieving specificity of mRNA decay through a promoter sequence and not a specific *cis* mRNA sequence, as shown for *SWI5* and *CLB2*, is a unique attribute. In order to maintain coordination between transcription and cytoplasmic decay, only the promoter sequence needs to be conserved, whereas the mRNA sequence can vary independently without disrupting regulation of either process. If multiple genes share promoter sequences, the entire expression process can be coordinated as a group. For example, *SWI5* and *CLB2* share promoter sequences with 33 other genes in the *CLB2* cluster involved in the G2/M transition (Koranda et al., 2000; Spellman et al., 1998; Zhu et al., 2000) and may be similarly regulated. Several of these genes are toxic when overexpressed (Niu et al., 2008; Sopko et al., 2006), indicating that timing of their expression during the cell cycle is restricted. Such coordination would ensure that all mRNAs in a group would oscillate as one entity, ensuring sharp transitions between cell-cycle phases. It is possible that the promoter-dependent coordination between transcription and mRNA decay could be employed by cell-cycle cluster genes other than the *CLB2* (there are eight in budding yeast; Spellman et al. [1998]). Interestingly, several transcripts in budding yeast couple the regulation of their stability with the transcriptional activity of RNAPII through polymerase-interacting subunits Rbp4/7 (Goler-Baron et al., 2008). This coupling phenomenon is employed by ~10% of the genes in

Saccharomyces cerevisiae and was shown to be preserved through evolution (Dori-Bachash et al., 2011). Thus, intriguingly, promoter-dependent regulation of mRNA stability could be a common strategy of control of mRNAs turnover in yeast and possibly in a variety of eukaryotic cells.

SWI5 and *CLB2* mRNA Life Cycle

We propose a model whereby the regulation of cytoplasmic *SWI5* and *CLB2* mRNA decay begins concurrently with their transcription (Figure 7). To provide specificity of decay, independent of specific *cis* mRNAs sequences, the decay regulator must be recruited by *SWI5* and *CLB2* transcription factors to their promoters and deposited onto the mRNA during transcription. Possibly, the promoter recruits factors that influence a specific mRNA feature, such as the cap structure, the poly(A) tail, or their associated proteins. We identified Dbf2p kinase as a regulator of *SWI5* and *CLB2* decay and found it associated with their mRNAs during transcription. *SWI5* and *CLB2* are additionally stabilized by Dbf20p. Unlike Dbf2p, Dbf20p does not bind to *SWI5* and *CLB2* cotranscriptionally and likely associates with mRNAs in the cytoplasm. Our data indicate therefore that, despite being redundant, Dbf2p and Dbf20p have distinct functions in regulation of *SWI5* and *CLB2* mRNA stability, indicating that their roles in the decay process are complex and could involve multiple regulators.

How Dbf2p becomes recruited to the promoters of *SWI5* and *CLB2* and how the two kinases interact with the mRNAs is not clear. Interaction of Dbf2p with Cdc5p (Visintin and Amon, 2001), a *SWI5* and *CLB2* transcription factor (Darieva et al., 2006), suggests a possible mechanism. Additionally, the mechanism whereby Dbf2p and Dbf20p regulate mRNA stability is also unknown. This regulation is independent of Dbf2p (and presumably Dbf20p) kinase activity, which is triggered shortly after metaphase-to-anaphase transition to promote progression from telophase to G1 phase (Toyn and Johnston, 1994). These results are consistent with our findings that Dbf2p and Dbf20p stabilize *SWI5* and *CLB2* mRNAs prior to mitosis when their kinase activity is low (Toyn and Johnston, 1994). Because the prometaphase/metaphase and anaphase are separated only by a couple of minutes, it is possible that insufficient time resolution during mitosis obscured precisely when the mRNA stability switch occurs. Nevertheless, our data indicate that Dbf2p and Dbf20p have two biologically distinct and mutually independent functions: one involved in regulation of mRNA stability described here and a better understood one involved in the regulation of completion of mitosis as MEN regulators (Mah et al., 2001).

Additionally, how Dbf2p and Dbf20p relay cell-cycle signals onto the mRNA decay machinery to initiate decay remains to be determined. Dbf2p is dephosphorylated during mitosis (Toyn and Johnston, 1994), and we speculate that this dephosphorylation event could act as a cell-cycle signal, thereby synchronizing mRNA degradation and mitotic division. Intriguingly, association of Dbf2p with the CCR4-NOT complex suggests that regulation of decay could be manifested through the regulation of deadenylation, as determined for tristetraprolin protein TTP. Dephosphorylation of TTP controls if and when CCR4-NOT complex is able to gain access to the mRNA to initiate decay (Clement et al., 2011; Sandler et al., 2011). Similarly to TTP, Dbf2p and Dbf20p might regulate accessibility of CCR4-NOT complex to the *SWI5* and *CLB2* mRNAs in a dephosphorylation-dependent but kinase activity-independent manner.

Here, we show that the fate of the *SWI5* and *CLB2* mRNA is determined cotranscriptionally at their birth. Thus, the decay marker assembles on the mRNA and is exported with it into the cytoplasm, priming the mRNAs for immediate decay once a cell-cycle signal arrives. Furthermore, in budding yeast, transcriptional activity can directly determine how an mRNA will localize, translate, and degrade in the cytoplasm (Harel-Sharvit et al., 2010; Shen et al., 2010). Thus, we hypothesize that a subset of yeast mRNAs could become "fully functionally configured" during their synthesis. These mRNAs could exit the nucleus equipped with the regulatory proteins that would define their translation, localization, and decay, which would then be "shed away" from an mRNA in a step-by-step manner after each completed step (Trcek and Singer, 2010). This model of mRNP formation is quite different from the one generally assumed for an mRNA, wherein proteins that regulate different steps in an mRNA life path interact with an mRNA only when their function is needed (Balagopal and Parker, 2009). Our study may thus have far-reaching implications that will serve as a platform for the analysis of mRNA decay and proteins that regulate it in a variety of mRNAs and organisms.

EXPERIMENTAL PROCEDURES

Yeast Strains

Table S3 and the Extended Experimental Procedures list yeast strains used and their synchronization and growth conditions.

FISH Probes and Procedure

Per gene, three to seven probes were used, each labeled with > 90% labeling efficiency (Table S1). Design, synthesis, and labeling of probes were performed as described previously (Femino et al., 2003; Zenklusen et al., 2008).

ACT1 mRNA was highly expressed, and therefore reliable counting of single transcripts in a maximal projection as performed for *SWI5* and *CLB2* was not possible. Instead, images were sum projected, and total fluorescent intensity of *ACT1* FISH signal for each cell was measured and presented as an average. The summed fluorescent values were corrected for the autofluorescent cellular background of the same cellular size from the control cells not hybridized with *ACT1* probes. The control cells were subjected to the same hybridization procedure and imaged as *ACT1* FISH cells only without the *ACT1* probes.

Mathematical Model

The number of transcripts measured in a particular phase of the cell cycle is the time-integrated average of the time-dependent solution (Equation 2) divided by the length of that particular cell-cycle phase:

$$\langle N \rangle = \left(\frac{1}{kT_c}\right)\left[\left(\frac{m}{kT} - N_0\right)\left(e^{-kT} - 1\right) + \left(\frac{mT_c}{T}\right)\right] \quad (3)$$

where brackets denote the ensemble average over the population of cells in a particular cell-cycle phase; T_c is the duration of that phase; and m, T, and k are defined previously (Equation 2) as the number of nascent chains, the dwell time, and the decay rate, respectively. The initial number of transcripts N_0 is determined by the number of transcripts present at the end of the previous cell cycle stage:

$$N_{0_i} = N(T_{ci-1}, m_{i-1}, k_{i-1}, T) \quad (4)$$

where i designates the cell-cycle phase. Thus, the initial number of transcripts N_{0i} is determined from the time-dependent solution $N(t)$ (Equation 2) at a time

T_c corresponding to the length of the previous cell-cycle phase, where the kinetic values m_{i-1}, k_{i-1}, are also those of the previous cell-cycle phase. The dwell time (T) of a nascent chain at the gene is determined by the parameters v (RNAPII velocity) and l (transcript length) (see Tables S3 and S4). Equations 3 and 4 were used to model the data in Figures 3–6 and their supplemental data.

Table S4 summarizes the parameters used to model the FISH data. For WT *SWI5*, *CLB2*, *SWI5* with *ACT1* 5′ and 3′UTRs, and *DOA1* expressed from the *SWI5* promoter, the mitotic decay was measured by fitting their cytoplasmic mRNA abundances after anaphase onset to an exponential decay with a single component. A slow decay was determined by calculating a global nonlinear least-square fit to the N and m with two floating parameters (T and a premitotic decay rate), and the mitotic decay (from P/M to T/C) rate measured by FISH was fixed.

For WT *DOA1*, *SWI5* expressed from the *ACT1* promoter, *SWI5* with *ACT1* 5′ and 3′UTRs expressed from the *ACT1* promoter, and *CLB2* expressed from the *ACT1* promoter, the data with one free parameter (a single k) were modeled. The velocity v of the RNAPII of 33 bp/s was assumed (Mason and Struhl, 2005) to obtain the dwell time T of 68 s (WT *DOA1*), 72 s (*SWI5* with an *ACT1* promoter), 70 s (*SWI5* with *ACT1* 5′ and 3′UTRs expressed from the *ACT1* promoter), and 66 s (*CLB2* with an *ACT1* promoter).

For *ΔDbf2* and *ΔDbf20* deletions, for *DOA1* mRNA expressed from a *CLB2* promoter, and for the Dbf2p kinase dead experiment, the mitotic decay could not be determined directly from their cytoplasmic mRNA profiles because, in these strains, the mitotic phases were extended two to three times relative to WT, and the addition of new mRNAs due to ongoing transcription was not negligible. Here, the data were modeled with the fixed T of 66 s for *SWI5*, 63 s for *CLB2*, and 77 s for *DOA1* determined for the WT *SWI5* and *CLB2*, respectively, whereas the premitotic and mitotic decay rates were free parameters.

Identification of Dbf2p and Dbf20p as *SWI5* and *CLB2* Decay Regulators

A bona fide regulator of *SWI5* and *CLB2* decay requires interaction with their transcription factors, the mRNA decay regulators, and the cell-cycle machinery to ensure coordination among the three. Cell cycle-dependent transcription of *SWI5* and *CLB2* is regulated by four transcription factors (Ndd1p, Fkh2p, Mcm1p, and Cdc5p), and their promoter binding positions have been determined (Darieva et al., 2006; Koranda et al., 2000; Spellman et al., 1998; Zhu et al., 2000). We reasoned that, because the stability of *SWI5* and *CLB2* is promoter specified, the mRNA decay regulator that we were searching for has to be recruited to *SWI5* and *CLB2* promoters by one of their transcription factors to ensure specificity of decay. This regulator, in turn, has to interact or be a part of the mRNA decay machinery and the cell-cycle progression machinery to further enable the coordination of decay through mitotic division.

In the search of this *trans*-acting factor, we made use of the *Saccharomyces* genome database. Ndd1p, Fkh2p, Mcm1p, and Cdc5p each uniquely interacted with 5, 14, 20, and 97 proteins, respectively. Dbf2p, a mitotic exit network (MEN) kinase, was the only protein that satisfied our criterion; it interacts with Cdc5p (Visintin and Amon, 2001), a *SWI5* and *CLB2* transcription factor and itself a MEN regulator (Darieva et al., 2006). It is furthermore a part of a larger 1.9 MDa CCR4-NOT complex (Liu et al., 1997), a major deadenylase of cytoplasmic mRNAs in yeast (Tucker et al., 2001), and it is mitotically active to ensure telophase-to-G1 phase transition (Toyn and Johnston, 1994).

Dbf2p interacts with four out of nine proteins of the CCR4-NOT complex: with Ccr4p, the catalytic subunit of CCR4-NOT complex with deadenylase activity (Tucker et al., 2002); with Pop2p, Caf40p, and Caf36p, noncatalytic subunits of CCR4-NOT complex; and also with Caf4p, a CCR4-NOT-associated protein; and with Cdc33p and Cdc20p, a 5′ cap-binding protein and a cap-associated protein. Dbf2p copurifies with all components of the complex itself and coimmunoprecipitates with the Ccr4p and Pop2p proteins (Liu et al., 1997). Additionally, *ΔDBF2* results in similar phenotypes and transcriptional defects to those observed in *ΔCCR4* and *ΔPOP2*. Conversely, *ΔCCR4* and *ΔPOP2* affected mitotic cell-cycle progression similar to that observed for *ΔDBF2*, indicating that Ccr4p, Pop2p, and Dbf2p all participate in regulating gene expression and cell-cycle progression during late mitosis (Liu et al., 1997).

Dbf2p is synthetically lethal with Dbf20p, which is not known to interact with the CCR4-NOT complex or Cdc5p like Dbf2p. During the cell cycle, however, Dbf20p performs several Dbf2p functions (Toyn et al., 1991), so we assayed the role of Dbf20p in regulation of *SWI5* and *CLB2* mRNA decay as well.

Apart from Dbf2p, *SWI5* and *CLB2* transcription factors displayed other interactions—but either with the major mRNA decay regulators or cell-cycle progression regulators and not both, thus making them unsuitable candidates. For example, Mcm1p interacted with Arg81p, and Cdc5p interacted with Cse4p that, in turn, interacted with Dcp2p, a catalytic subunit of the Dcp1p-Dcp2p decapping enzyme complex. Cdc5p also interacted with Mcd1p that, in turn, interacted with Not5p, a subunit of the CCR4-NOT complex and with Nop13p and Pds5p that, in turn, interacted with Xrn1p, a 5'-3' exonuclease and a component of cytoplasmic processing (P) bodies involved in mRNA decay.

Finally, apart from its role as a transcription factor, Cdc5p is mostly known as a MEN regulator in promoting transition of cells from telophase into G1 phase (Toyn and Johnston, 1994). It physically interacts with several MEN regulators, for example, with Dbf2p. Unlike Dbf2p however, none of these regulators, in turn, interact with the mRNA decay factors, making these proteins unsuitable candidates involved in the regulation of *SWI5* and *CLB2* mRNA stability.

Unless cited, the protein descriptions were obtained from the *Saccharomyces* genome database.

Chromatin Immunoprecipitation and RNA Immunoprecipitation

45 ml of cells were grown in YPD until OD_{600} ~0.35. Cells were synchronized in S or M phase with HU (see Extended Experimental Procedures). Chromatin immunoprecipitation (ChIP) was performed as described in Moldón et al. (2008) and Table S5. For RNase ChIP in mitotic cells, crosslinked extracts were treated with DNase-free RNase (50 μg/ml, Roche) for 15 min at 37°C prior to sonication. RNA immunoprecipitation was performed as described in Gilbert et al. (2004).

Measuring mRNA Decay Rates Using qRT-PCR and Thiolutin

See Table S6 and the accompanying text.

SUPPLEMENTAL INFORMATION

Supplemental Information includes Extended Experimental Procedures, six figures, and six tables and can be found with this article online at doi:10.1016/j.cell.2011.11.051.

ACKNOWLEDGMENTS

We would like to thank Drs. Jeffrey Chao and Kevin Czaplinski for helpful discussion of the project and Xiuhua Meng for her help with cloning. We thank Drs. Ian Willis, Michael Keogh, and Angelika Amon for sharing *ΔSWI5* (TT012), Pab1p-TAP (TT065) strains, and Dbf2p-kinase dead plasmid with us, respectively. This work was supported by an EMBO fellowship awarded to A.M., GM57829 to C.C.Q., and GM57071 to R.H.S.

Received: December 6, 2010
Revised: July 27, 2011
Accepted: November 22, 2011
Published: December 22, 2011

REFERENCES

Ardehali, M.B., and Lis, J.T. (2009). Tracking rates of transcription and splicing in vivo. Nat. Struct. Mol. Biol. *16*, 1123–1124.

Balagopal, V., and Parker, R. (2009). Polysomes, P bodies and stress granules: states and fates of eukaryotic mRNAs. Curr. Opin. Cell Biol. *21*, 403–408.

Bean, J.M., Siggia, E.D., and Cross, F.R. (2006). Coherence and timing of cell cycle start examined at single-cell resolution. Mol. Cell *21*, 3–14.

Brewer, B.J., Chlebowicz-Sledziewska, E., and Fangman, W.L. (1984). Cell cycle phases in the unequal mother/daughter cell cycles of Saccharomyces cerevisiae. Mol. Cell. Biol. *4*, 2529–2531.

Cai, T., Aulds, J., Gill, T., Cerio, M., and Schmitt, M.E. (2002). The Saccharomyces cerevisiae RNase mitochondrial RNA processing is critical for cell cycle progression at the end of mitosis. Genetics *161*, 1029–1042.

Clement, S.L., Scheckel, C., Stoecklin, G., and Lykke-Andersen, J. (2011). Phosphorylation of tristetraprolin by MK2 impairs AU-rich element mRNA decay by preventing deadenylase recruitment. Mol. Cell. Biol. *31*, 256–266.

Darieva, Z., Bulmer, R., Pic-Taylor, A., Doris, K.S., Geymonat, M., Sedgwick, S.G., Morgan, B.A., and Sharrocks, A.D. (2006). Polo kinase controls cell-cycle-dependent transcription by targeting a coactivator protein. Nature *444*, 494–498.

Dori-Bachash, M., Shema, E., and Tirosh, I. (2011). Coupled evolution of transcription and mRNA degradation. PLoS Biol. *9*, e1001106.

Femino, A.M., Fay, F.S., Fogarty, K., and Singer, R.H. (1998). Visualization of single RNA transcripts in situ. Science *280*, 585–590.

Femino, A.M., Fogarty, K., Lifshitz, L.M., Carrington, W., and Singer, R.H. (2003). Visualization of single molecules of mRNA in situ. Methods Enzymol. *361*, 245–304.

Fitch, I., Dahmann, C., Surana, U., Amon, A., Nasmyth, K., Goetsch, L., Byers, B., and Futcher, B. (1992). Characterization of four B-type cyclin genes of the budding yeast Saccharomyces cerevisiae. Mol. Biol. Cell *3*, 805–818.

Gilbert, C., Kristjuhan, A., Winkler, G.S., and Svejstrup, J.Q. (2004). Elongator interactions with nascent mRNA revealed by RNA immunoprecipitation. Mol. Cell *14*, 457–464.

Gill, T., Cai, T., Aulds, J., Wierzbicki, S., and Schmitt, M.E. (2004). RNase MRP cleaves the CLB2 mRNA to promote cell cycle progression: novel method of mRNA degradation. Mol. Cell. Biol. *24*, 945–953.

Goler-Baron, V., Selitrennik, M., Barkai, O., Haimovich, G., Lotan, R., and Choder, M. (2008). Transcription in the nucleus and mRNA decay in the cytoplasm are coupled processes. Genes Dev. *22*, 2022–2027.

Grigull, J., Mnaimneh, S., Pootoolal, J., Robinson, M.D., and Hughes, T.R. (2004). Genome-wide analysis of mRNA stability using transcription inhibitors and microarrays reveals posttranscriptional control of ribosome biogenesis factors. Mol. Cell. Biol. *24*, 5534–5547.

Guhaniyogi, J., and Brewer, G. (2001). Regulation of mRNA stability in mammalian cells. Gene *265*, 11–23.

Harel-Sharvit, L., Eldad, N., Haimovich, G., Barkai, O., Duek, L., and Choder, M. (2010). RNA polymerase II subunits link transcription and mRNA decay to translation. Cell *143*, 552–563.

Hartwell, L.H. (1974). Saccharomyces cerevisiae cell cycle. Bacteriol. Rev. *38*, 164–198.

Holstege, F.C., Jennings, E.G., Wyrick, J.J., Lee, T.I., Hengartner, C.J., Green, M.R., Golub, T.R., Lander, E.S., and Young, R.A. (1998). Dissecting the regulatory circuitry of a eukaryotic genome. Cell *95*, 717–728.

Jimenez, A., Tipper, D.J., and Davies, J. (1973). Mode of action of thiolutin, an inhibitor of macromolecular synthesis in Saccharomyces cerevisiae. Antimicrob. Agents Chemother. *3*, 729–738.

Koranda, M., Schleiffer, A., Endler, L., and Ammerer, G. (2000). Forkhead-like transcription factors recruit Ndd1 to the chromatin of G2/M-specific promoters. Nature *406*, 94–98.

Larson, D.R., Johnson, M.C., Webb, W.W., and Vogt, V.M. (2005). Visualization of retrovirus budding with correlated light and electron microscopy. Proc. Natl. Acad. Sci. USA *102*, 15453–15458.

Larson, D.R., Zenklusen, D., Wu, B., Chao, J.A., and Singer, R.H. (2011). Real-time observation of transcription initiation and elongation on an endogenous yeast gene. Science *332*, 475–478.

Liu, H.Y., Toyn, J.H., Chiang, Y.C., Draper, M.P., Johnston, L.H., and Denis, C.L. (1997). DBF2, a cell cycle-regulated protein kinase, is physically and functionally associated with the CCR4 transcriptional regulatory complex. EMBO J. *16*, 5289–5298.

Lord, P.G., and Wheals, A.E. (1980). Asymmetrical division of Saccharomyces cerevisiae. J. Bacteriol. *142*, 808–818.

Mah, A.S., Jang, J., and Deshaies, R.J. (2001). Protein kinase Cdc15 activates the Dbf2-Mob1 kinase complex. Proc. Natl. Acad. Sci. USA *98*, 7325–7330.

Marzluff, W.F., Wagner, E.J., and Duronio, R.J. (2008). Metabolism and regulation of canonical histone mRNAs: life without a poly(A) tail. Nat. Rev. Genet. *9*, 843–854.

Mason, P.B., and Struhl, K. (2005). Distinction and relationship between elongation rate and processivity of RNA polymerase II in vivo. Mol. Cell *17*, 831–840.

Moldón, A., Malapeira, J., Gabrielli, N., Gogol, M., Gómez-Escoda, B., Ivanova, T., Seidel, C., and Ayté, J. (2008). Promoter-driven splicing regulation in fission yeast. Nature *455*, 997–1000.

Niu, W., Li, Z., Zhan, W., Iyer, V.R., and Marcotte, E.M. (2008). Mechanisms of cell cycle control revealed by a systematic and quantitative overexpression screen in S. cerevisiae. PLoS Genet. *4*, e1000120.

Osley, M.A. (1991). The regulation of histone synthesis in the cell cycle. Annu. Rev. Biochem. *60*, 827–861.

Passos, D.O., and Parker, R. (2008). Analysis of cytoplasmic mRNA decay in Saccharomyces cerevisiae. Methods Enzymol. *448*, 409–427.

Pelechano, V., and Pérez-Ortín, J.E. (2008). The transcriptional inhibitor thiolutin blocks mRNA degradation in yeast. Yeast *25*, 85–92.

Sandler, H., Kreth, J., Timmers, H.T., and Stoecklin, G. (2011). Not1 mediates recruitment of the deadenylase Caf1 to mRNAs targeted for degradation by tristetraprolin. Nucleic Acids Res. *39*, 4373–4386.

Shen, Z., St-Denis, A., and Chartrand, P. (2010). Cotranscriptional recruitment of She2p by RNA pol II elongation factor Spt4-Spt5/DSIF promotes mRNA localization to the yeast bud. Genes Dev. *24*, 1914–1926.

Sopko, R., Huang, D., Preston, N., Chua, G., Papp, B., Kafadar, K., Snyder, M., Oliver, S.G., Cyert, M., Hughes, T.R., et al. (2006). Mapping pathways and phenotypes by systematic gene overexpression. Mol. Cell *21*, 319–330.

Spellman, P.T., Sherlock, G., Zhang, M.Q., Iyer, V.R., Anders, K., Eisen, M.B., Brown, P.O., Botstein, D., and Futcher, B. (1998). Comprehensive identification of cell cycle-regulated genes of the yeast Saccharomyces cerevisiae by microarray hybridization. Mol. Biol. Cell *9*, 3273–3297.

Talarek, N., Cameroni, E., Jaquenoud, M., Luo, X., Bontron, S., Lippman, S., Devgan, G., Snyder, M., Broach, J.R., and De Virgilio, C. (2010). Initiation of the TORC1-regulated G0 program requires Igo1/2, which license specific mRNAs to evade degradation via the 5′-3′ mRNA decay pathway. Mol. Cell *38*, 345–355.

Toyn, J.H., Araki, H., Sugino, A., and Johnston, L.H. (1991). The cell-cycle-regulated budding yeast gene DBF2, encoding a putative protein kinase, has a homologue that is not under cell-cycle control. Gene *104*, 63–70.

Toyn, J.H., and Johnston, L.H. (1994). The Dbf2 and Dbf20 protein kinases of budding yeast are activated after the metaphase to anaphase cell cycle transition. EMBO J. *13*, 1103–1113.

Trcek, T., and Singer, R.H. (2010). The cytoplasmic fate of an mRNP is determined cotranscriptionally: exception or rule? Genes Dev. *24*, 1827–1831.

Tucker, M., Valencia-Sanchez, M.A., Staples, R.R., Chen, J., Denis, C.L., and Parker, R. (2001). The transcription factor associated Ccr4 and Caf1 proteins are components of the major cytoplasmic mRNA deadenylase in Saccharomyces cerevisiae. Cell *104*, 377–386.

Tucker, M., Staples, R.R., Valencia-Sanchez, M.A., Muhlrad, D., and Parker, R. (2002). Ccr4p is the catalytic subunit of a Ccr4p/Pop2p/Notp mRNA deadenylase complex in Saccharomyces cerevisiae. EMBO J. *21*, 1427–1436.

Visintin, R., and Amon, A. (2001). Regulation of the mitotic exit protein kinases Cdc15 and Dbf2. Mol. Biol. Cell *12*, 2961–2974.

Wang, Y., Liu, C.L., Storey, J.D., Tibshirani, R.J., Herschlag, D., and Brown, P.O. (2002). Precision and functional specificity in mRNA decay. Proc. Natl. Acad. Sci. USA *99*, 5860–5865.

Zenklusen, D., Larson, D.R., and Singer, R.H. (2008). Single-RNA counting reveals alternative modes of gene expression in yeast. Nat. Struct. Mol. Biol. *15*, 1263–1271.

Zhu, G., Spellman, P.T., Volpe, T., Brown, P.O., Botstein, D., Davis, T.N., and Futcher, B. (2000). Two yeast forkhead genes regulate the cell cycle and pseudohyphal growth. Nature *406*, 90–94.